Eur. Phys. J. D **44**, 301–305 (2007)
DOI: 10.1140/epjd/e2007-00142-5

THE EUROPEAN PHYSICAL JOURNAL D

Measurements of sound velocity of laser-irradiated iron foils relevant to Earth core condition

K. Shigemori[1,a], D. Ichinose[1], T. Irifune[2], K. Otani[1], T. Shiota[1], T. Sakaiya[1], and H. Azechi[1]

[1] Institute of Laser Engineering, Osaka University, Suita, Osaka 565-0871, Japan
[2] Geodynamics Research Center, Ehime University, Matsuyama, Ehime 790-8577, Japan

Received 16 February 2006 / Received in final form 6 December 2006
Published online 6 April 2007 –

Abstract. We present a novel scheme to measure sound velocity of shock-compressed iron of geophysical interest. The sound velocity of laser-irradiated iron foils was obtained with side-on X-ray radiograph technique from measured rarefaction wave velocity of shocked iron. Iron foils were irradiated with a two-stepped square laser pulse to reach Earth's core condition by double compression. The experimental parameters of temperature and pressure were very close to the Earth's core condition.

PACS. 52.35.Tc Shock waves and discontinuities – 91.35.-x Earth's interior structure and properties – 52.50.Jm Plasma production and heating by laser beams (laser-foil, laser-cluster, etc.) – 52.70.La X-ray and gamma-ray measurements

1 Introduction

The Earth's core has a radius of ∼3000 km, which is approximately the half of the Earth's radius. From many seismological studies, it is suggested that the outer Earth core is liquid, and the inner core is solid. The Earth core is composed of iron-nickel alloy [1] with some fractions of light elements such as hydrogen, oxygen, silicon, and so forth. The temperature and the pressure of the Earth's center are estimated to be 5000–7000 K and 360 GPa, respectively [1,2]. However, there have been still significant uncertainties in these estimates. The parameters relevant to the Earth's core, such as temperature, pressure, density are of great importance for study of the structure and the evolution of the Earth.

The experimental studies on iron under high pressure have been done mainly by static compression technique by means of diamond anvil cells (DACs). The maximum pressure by the DAC is above the Earth center pressure, but it is very difficult to increase temperature up to the Earth core condition by technical problems on DACs. Some works on the equation of state of iron have been done under high pressure with intense lasers [3–5] as well as gas guns [6,7].

Among physical parameters of the Earth's core, the sound velocity is the most important parameter because it can be directly compared with huge seismological data. Previous experimental studies on the iron sound velocity were carried out with gas guns. Brown and McQueen showed the first experimental data of iron at the pressure of the Earth's core [6]. The sound velocity increases as a function of pressure, but there was clear discontinuity at pressures around 250 GPa. This discontinuity was interpreted by a solid-solid phase transition in iron near these pressures. Recent experimental results by Nguyen and Holmes also showed the discontinuous change in the sound velocity at around 250 GPa [7]. However, they interpreted this was caused by melting of iron at these pressures. Although there are some experimental investigations on the melting of iron at high pressure [8,9], these melting curves are apparently different from those by theoretical calculations [10,11]. Nevertheless, more recent calculations show mutually consistent results, suggesting that the melting temperature is around 6000 K at 250 GPa [12–16]. Previous gas-gun experiments were basically done with a single-shock compression, so that the temperature of the shock compressed region should lie on the principal Hugoniot curve. The Hugoniot temperature curve crosses the melting curves at around 6000 K and 250 GPa; this is the reason why the discontinuity in the sound velocity was supposed to be due to melting, because the liquid sound velocity is lower than the solid sound velocity. This fact also indicates that it is impossible to obtain the solid sound velocity data above 250 GPa by the single-shock compression.

In this paper, we present the first measurements of iron sound velocity under the P, T conditions equivalent to the Earth's core by a double-shock compression with intense laser. We measured trajectories of the laser-irradiated surface and the rear surface in order to deduce the sound velocity in addition to pressure, density, shock velocity, and particle velocity by means of side-on X-ray backlighting technique. We also separately measured the temperature of the shocked iron foil by an

[a] e-mail: shige@ile.osaka-u.ac.jp

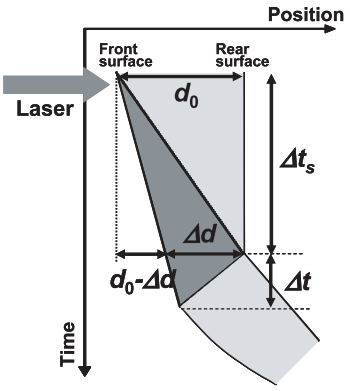

Fig. 1. A typical flow diagram of the laser-irradiated foils.

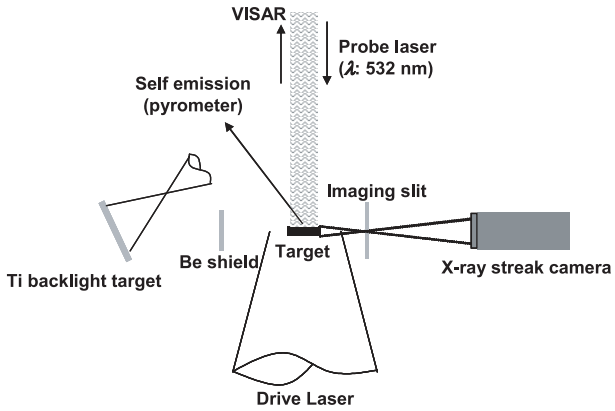

Fig. 2. Schematic view of the experimental setup.

optical pyrometer. The measured sound velocity was in good agreement with previous experimental results and calculation by one-dimensional simulation.

2 Measurement of sound velocity by X-ray backlighting technique

Measurements of the sound velocity of iron under high pressure had been carried out with optical instruments in previous gas gun experiments, using time difference of a stepped target with flyer plates [17]. We have developed a novel type of measurement to obtain the sound velocity and other important parameters of shock-compressed matter.

A typical flow diagram of the laser-irradiated foil is shown in Figure 1. When the foil is irradiated with intense laser, shock wave is generated and propagates into the foil. Once the shock front breaks out at the rear surface, rarefaction wave starts to move back to the laser-irradiated surface with its sound velocity. When the rarefaction front reaches the laser-irradiated surface, the whole foil begins to accelerate. The sound velocity of the shock-compressed region c_s is,

$$c_s = \Delta d/\Delta t, \tag{1}$$

where Δd is the shock-compressed thickness of the target at which the shock front reaches the rear surface, Δt is the time between the shock breakout and the rarefaction breakout. By time-resolved side-on X-ray radiograph [18], it is possible to obtain the two parameters from the trajectories of the both surfaces (edges). The side-on X-ray radiograph coupled with X-ray streak camera has been broadly used in hydrodynamic instability experiments and equation-of-states (EOS) experiments.

This measurement also provides several physical parameters of the shocked region. From the shock breakout timing Δt_s, we can obtain the averaged shock velocity, $u_s = d_0/\Delta t_s$, where d_0 is the initial target thickness, Δt_s is the shock breakout timing. The particle velocity u_p is also obtained from the trajectory of the laser-irradiated surface, which is written as

$$u_p = (d_0 - \Delta d)/\Delta t_s. \tag{2}$$

The compressibility is also determined as $d_0/\Delta d$. From the compressibility, it is possible to deduce the specific heat ratio γ and the density ρ_s. From these parameters, the shocked pressure P is obtained as

$$P = \rho_0 u_s u_p = \frac{\rho_s c_s}{\gamma}. \tag{3}$$

It is well-known that some parameters are determined by its Hugoniot curve for single shock compression from measured parameters by shock experiments. The calculated physical parameters shown above can be basically applied for off-Hugoniot conditions. This technique is very powerful tool not only for sound-velocity measurements but also for single-shot off-Hugoniot measurement.

3 Experiments

Experiments were done on the GEKKO-HIPER (High Intensity Plasma Experimental Research) laser facility [19] at the Institute of Laser Engineering, Osaka University. Iron foils were irradiated with two-stepped laser pulses. The foot pulse was partially coherent light [20] (PCL, λ: 0.53 μm, 2.3 ns) with an intensity of 1×10^{12} W/cm^2 followed by the main pulse, which was two-dimensionally smoothed by spectral dispersion [21] (SSD, λ: 0.35 μm, 2.6 ns) at an intensity of 2×10^{13} W/cm^2. In order to form a long pulse shape for the experiments, we stacked the foot and the main pulse beams with certain time delays. The stacked pulse durations of the foot pulse and the main pulse were 4 ns and 8 ns, respectively. We define the origin of the timing ($t = 0$) to be the half maximum of the rise time of the main drive pulse.

The targets were iron foils of 38-μm thickness. In laser-shock experiments, heating prior to the shock front due to radiation and hot electron is crucial. We placed a polystyrene (CH) ablator of ∼6-μm thickness on the laser-irradiated surface, and a gold insulator of 1-μm thickness was sandwiched between the iron foil and the CH ablator.

The sound velocity and the other important parameters were measured with side-on X-ray backlighting technique [18]. Schematic view of the experimental arrangement is shown in Figure 2. We employed a titanium (Ti) foil of 20-μm-thickness as a backlight target beside the

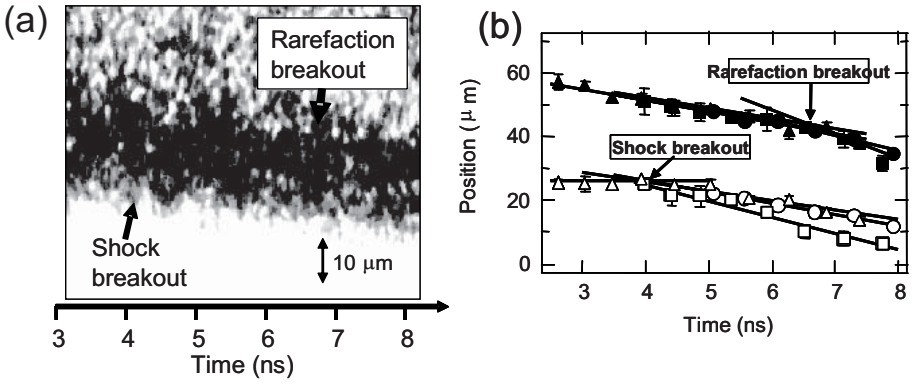

Fig. 3. (a) Raw streaked image of the laser irradiated iron foil by side-on X-ray radiograph. (b) Plots of the laser irradiated surface (closed symbols) and rear surface (open symbols).

iron foil in order to generate backlighting X-ray at the energy of ∼4.8 keV. The shadow of the iron foil from the side was imaged by a slit (10-μm width) onto a photocathode of an X-ray streak camera with a magnification of 22.5. The temporal resolution of the X-ray streak camera was ∼50 ps. The shocked temperature at the shock breakout timing was measured by a streaked optical spectral pyrometer [22]. We observed spatially-integrated (200-μm-diameter on the target) time-resolved spectra of optical self emission (λ: 380–560 nm) on the rear surface of the target. We deduced temperature from the optical spectra at the shock breakout. In addition to the pyrometer, we employed a velocity interferometer for any reflector (VISAR) [23]. We measured the shock velocity and the particle velocity by the VISAR in order to check the side-on X-ray backlighting measurement data. The shock velocity was measured with a wedged iron foil by the VISAR.

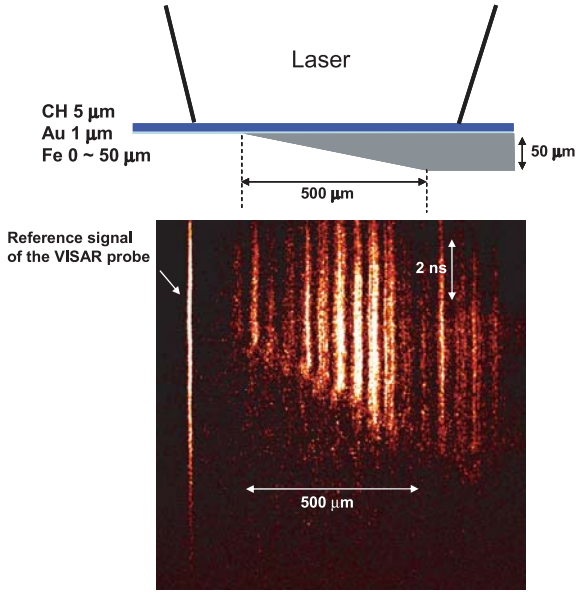

Fig. 4. (Color online) Raw image of the VISAR for the wedged target (0–50 μm).

4 Experimental results

Figure 3a is an example of raw streaked image of the X-ray backlighting measurement. From the raw data, we took temporally-integrated spatial lineouts of the emission for every 50 ps after a noise reduction. The edges where the intensity is at half maximum are determined as the trajectories of the laser-irradiated surface and the rear surface. In the side-on observation, there must be a problem of tilting of the foil from the observation angle. Although we employed relatively "narrow" envelope-shaped foils in order to avoid the tilting issue, there was a certain rotation of the target from the raw image because the observed foil thickness was larger than the initial thickness for some data shots. Since we observed 4.8 keV X-ray which does not pass through the iron, however, there is no problem to track the leading edges of the laser-irradiated iron foils except for the observation of low-density rarefaction tail. We analyzed the data taking into account the target tilting by the initial target thickness and the magnification of the diagnostics. The uncertainty of the tilting and presence of the gold layer were included in the error bars of the measured parameters. The effect on the error of the Au layer was less than 3%.

Figure 3b shows plots of the laser-irradiated surface and the rear surface from the X-ray radiograph measurements (three shots). We made linear fits to the trajectories for each experimental data. We determined the shock breakout timing from the crossing point of the initial target position (by linear fit at early timing) and the trajectory at the later timings (by linear fit at later timing) because the rear surface moves with a constant velocity after the shock breakout. Since the target tilting causes the systematic error of the expansion phase of the rarefaction tail, there are differences between each data shot. From the measured shock breakout timing, the averaged shock velocity u_s was ∼10.3 km/s. The shock front velocity was also measured by the VISAR with a wedged iron foil whose thickness was 0–40 μm. Figure 4 shows raw streaked image of the VISAR. The reflectivity decreases when the second main shock front passes at the rear surface, then the fringes rapidly disappear in accordance with the shape of the wedge because the direction of the shock front is not perpendicular to the rear surface. Although we observed the fringe shifts just after the shock breakout, we could not deduce the free surface velocity in good quality because the reflectivity just after the shock breakout is very

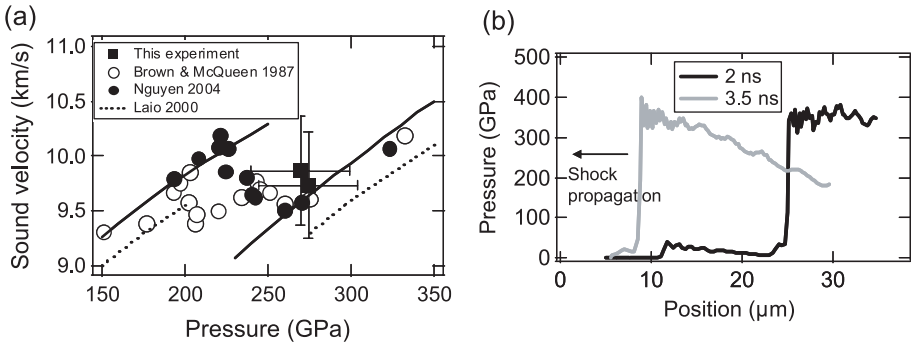

Fig. 5. Measured sound velocity in this in this experiment (squares) and previous gas gun data (circles). (b) Pressure profiles from one-dimensional simulation with ILESTA-1D code for different timings.

small. The shock velocity is obtained from the timings of the shock breakout to be ∼9.8 km/s. The shock breakout timing from the raw image suggests that the shock velocity is spatially and temporally constant within ∼10% fluctuation. Also, the measured shock velocity is very close to the radiograph measurement, indicating that the X-ray radiograph gives reasonable shock velocity. The measured shock velocity was also well reproduced by calculations with one-dimensional simulation ILESTA-1D [24].

We obtained the particle velocity u_p from the trajectory of the laser-irradiated surface by liner fit in early timing of the data. From linearly fitted line at the later timing, we obtained a crossing point as the rarefaction breakout timing, which is indicated in Figure 3b. From the time interval Δt and the shock-compressed thickness of the iron Δd, we deduced the sound velocity of the shock-compressed iron c_s. Also, we calculated the pressure P at the shock-compressed region from the measured parameters to be ∼270 GPa.

We also separately measured the shocked front temperature by the optical pyrometer from self-emission spectrum on the rear surface of the foil under the same laser irradiation condition [22]. The measured temperature was 6200 ± 500 K at the vicinity of the shock front for the shock breakout timing.

5 Discussions

Figure 5a shows the measured sound velocity from our experiments as well as previous experimental data with gas guns. Also shown in Figure 5a is calculated sound velocity on Hugoniot for solid and liquid irons. In general, the sound velocity (elastic sound velocity) for solid is higher than that for liquid because the solid sound velocity is determined by shear and bulk modulii, while liquid sound velocity is determined only by the shear modulus. Our experimental data are almost on the liquid Hugoniot curve even though we performed the double shock compression.

We calculated detailed parameters on the experiments by one-dimensional simulation ILESTA-1D. The basic parameters on hydrodynamics, i.e., the shock velocity, the particle velocity, and the sound velocity with the 1-D simulation calculation are in good agreements with the experimental results within an uncertainty of 10%. Since the foils were irradiated with the stacked laser pulse, however, the pulse shape was not absolutely flat-topped due to imperfection of the pulse stacking. The intensity "dip" between the pulses caused a small decompression in the iron foils. Figure 5b shows the calculated pressure profiles of the laser-irradiated iron for two different timings. The pressure profile at 2 ns, at the first main pulse timing, shows nearly uniform pressure profile. However, the pressure profile at the 3.5 ns, at the second pulse timing, shows significant decompression behind far the shock front. Thus we measured the sound velocity of different pressure regions (220–350 GPa) of the iron in the experiment, and the measured sound velocity and the pressure were "averaged" values in the shocked region. Note that the flow velocity (ablation surface velocity) does not dramatically change due to the decompression in this pressure region because the compression ratio does not change much. Thus, this is not a major reason of errors for analysis of the sound velocity.

We also found that these parameters (pressure, temperature) in the vicinity of the shock front are very close to those of the Earth's inner core. At the shock front position, the pressure and the temperature from the 1D simulation are approximately 350 GPa and 6600 K, respectively. The measured temperature is in good agreement with the simulation, which is below the single shock Hugoniot temperature at 350 GPa (∼9000 K). These values are also very close to previous double shock experiments [4]. By improving the pulse shaping and the pulse stacking, it is possible to obtain more spatially-uniform pressure and temperature condition relevant to the Earth's inner core.

6 Conclusion

In summary, we have performed the novel technique to measure the sound velocity under the P, T conditions relevant to Earth core with intense laser. We obtained the sound velocity of the shock-compresses iron as well as important parameters of the shocked iron by means of a side-on X-ray backlighting technique. The measured sound velocity of the high-pressure iron is very close to the previous experimental results with gas guns, showing "liquid" iron velocity. Although the measured sound velocity was of the shocked iron with pressure distribution due to the imperfection of the pulse shaping, this technique should provide a very promising way to address the key issues relevant to the Earth's core and other condensed matter physics.

The authors acknowledge many skillful technical staffs of laser operations, target fabrications, and plasma diagnostics at ILE, Osaka University.

References

1. F.J. Birch, J. Geophys. Res. **57**, 227 (1952)
2. A.M. Dziewonski, D.L. Anderson, Phys. Earth Planet. Inter. **25**, 297 (1981)
3. D. Batani, A. Morelli, M. Tomasini, A. Benuzzi-Mounaix, F. Philippe, M. Koenig, B. Marchet, I. Masclet, M. Rabec, Ch. Reverdin, R. Cauble, P. Celliers, G. Collins, L. Da Silva, T. Hall, M. Moret, B. Sacchi, P. Baclet, B. Cathala, Phys. Rev. Lett. **88**, 235502 (2002)
4. A. Benuzzi-Mounaix, M. Koenig, G. Huser, B. Faral, N. Grandjouan, D. Batani, E. Henry, M. Tomasini, T.A. Hall, F. Guyot, Phys. Rev. E **70**, 045401(R) (2004)
5. G. Huser, M. Koenig, A. Benuzzi-Mounaix, E. Henry, T. Vinci, B. Faral, M. Tomasini, B. Telano, D. Batani, Phys. Plasmas **12**, 60701 (2005)
6. J.M. Brown, R.J. McQueen, J. Geophys. Res. **91**, 7485 (1986)
7. J.H. Nguyen, N.C. Holmes, Nature **427**, 339 (2004)
8. C.S. Yoo, N.C. Holmes, M. Ross, D.J. Webb, C. Pike, Phys. Rev. Lett. **70**, 3931 (1993)
9. R. Boehler, Nature **363**, 534 (1993)
10. M. Ross, D.A. Young, R. Grover, J. Geophys. Lett. **95**, 21713 (1990)
11. Q. Williams, E. Knittle, R. Jeanloz, J. Geophys. Res. **96**, 2171 (1991)
12. T.J. Ahrens, K.G. Holland, C.Q. Chen, Geophys. Res. Lett. **29**, 54-1 (2002)
13. D. Alfè, M.J. Gillan, G.D. Price, Nature **401**, 462 (1999)
14. A. Laio, S. Bernard, G.D. Chiarotti, S. Scandolo, E. Tosatti, Science **287**, 1027 (2000)
15. A.B. Belonoshko, R. Ahuja, B. Johansson, Phys. Rev. Lett. **84**, 3638 (2000)
16. D. Alfè, G.D. Price, M.J. Gillan, Phys. Rev. B **65**, 165118 (2002)
17. R.J. McQueen, J.W. Hopson, J.N. Flitz, Rev. Sci. Instrum. **53**, 245 (1982)
18. K. Shigemori, H. Azechi, M. Nakai, M. Honda, K. Meguro, N. Miyanaga, H. Takabe, K. Mima, Phys. Rev. Lett. **78**, 250 (1997); S. Fujioka, H. Shiraga, M. Nishikino, Y. Tamari, K. Shigemori, M. Nakai, H. Azechi, K.A. Tanaka, T. Yamanaka, Rev. Sci. Instrum. **74**, 2198 (2003)
19. N. Miyanaga et al., *IAEA Fusion Energy Conference*, Sorrento, Italy, IAEA-CN-77 (2000)
20. H. Nakano, N. Miyanaga, K. Yagi, K. Tsubakimoto, T. Kanabe, M. Nakatsuka, S. Nakai, Appl. Phys. Lett. **63**, 580 (1993)
21. S. Skupsky, R.W. Short, T. Kesler, R.S. Craxton, S. Letzing, J. M. Soures, J. Appl. Phys. **66**, 3456 (1989)
22. K. Shigemori, K. Otani, T. Shiota, H. Azechi, K. Mima, Jpn J. Appl. Phys. **45**, 4224 (2006)
23. L.M. Barker, R.E. Hollenbach, Appl. Phys. Lett. **43**, 4669 (1972)
24. H. Takabe, M. Yamanaka, K. Mima, C. Yamanaka, H. Azechi, N. Miyanaga, M. Nakatsuka, T. Jitsuno, T. Norimatsu, M. Takagi, H. Nishimura, M. Nakai, T. Yabe, T. Sasaki, K. Yoshida, K. Nishihara, Y. Kato, Y. Izawa, T. Yamanaka, S. Nakai, Phys. Fluids **31**, 2884 (1988)